

How does Spreading Depression Spread? - Physiology and Modeling

Bas-Jan Zandt,^{1, a)} Bennie ten Haken,² Michel J.A.M. van Putten,^{2,3} and Markus A. Dahlem⁴

¹⁾Department of Biomedicine, University of Bergen, Bergen, Norway

²⁾MIRA-Institute for Biomedical Technology and Technical Medicine, University of Twente, Enschede, the Netherlands

³⁾Department of Clinical Neurophysiology, Medisch Spectrum Twente, Enschede, the Netherlands

⁴⁾Department of Physics, Humboldt-Universität zu Berlin, Berlin, Germany.

Spreading depression (SD) is a wave phenomenon in gray matter tissue. Locally, it is characterized by massive re-distribution of ions across cell membranes. As a consequence, there is a sustained membrane depolarization and tissue polarization that depresses any normal electrical activity. Despite these dramatic cortical events, SD remains difficult to observe in humans noninvasively, which for long has slowed advances in this field. The growing appreciation of its clinical importance in migraine and stroke is therefore consistent with an increasing need for computational methods that tackle the complexity of the problem at multiple levels. In this review, we focus on mathematical tools to investigate the question of spread and its two complementary aspects: What are the physiological mechanisms and what is the spatial extent of SD in the cortex? This review discusses two types of models used to study these two questions, namely Hodgkin-Huxley type and generic activator-inhibitor models, and the recent advances in techniques to link them.

Keywords: propagation; reaction-diffusion; migraine; excitable medium; potassium; dynamics

I. INTRODUCTION AND SCOPE

Spreading depression (SD), or depolarization¹, is a slowly traveling wave (mm/min) characterized by neuronal depolarization and redistribution of ions between the intra- and extracellular space, that temporarily depresses electrical activity², see Figure I. The phenomenon occurs in many neurological conditions, such as migraine with aura, ischemic stroke, traumatic brain injury and possibly epilepsy^{3,4}. Migraine is the most prevalent condition in which SD occurs and causes significant disability⁵. SD seems to be relatively harmless for the neural tissue in the case of migraine aura, where a functional increase in blood flow enables a fast recovery. SD also occurs in ischemic stroke, where it can aggravate ischemic damage and its occurrence has been shown to correlate with poor outcome^{6,7}.

SD is a reaction-diffusion (RD) process, similar to the propagation of a flame on a matchstick⁸. SD consists of local “reaction” processes, such as release of potassium and glutamate, pump activity and recovery of the tissue in a later stage, as well as diffusion of potassium and glutamate, which enables the propagation of SD. Knowledge of the local dynamics and propagation of SD is essential for designing successful therapies that prevent or halt migraine attacks, or protect tissue in the penumbra from secondary damage after ischemic stroke.

Modeling cardiac arrhythmia serves as example

Research in the last five decades, starting with the seminal work of Wiener and Rosenblueth⁹, has shown that cardiac arrhythmias can be explained in terms of nonlinear RD wave dynamics in 2D (or 3D). Whole heart computer models of arrhythmia can predict what happens to the heart, and they led to the development of new medical strategies¹⁰. On the cellular level, models of action potentials in cardiac cells also incorporate ion dynamics, for example, to model cardiac beat-to-beat variations and higher-order rhythms in ischemic ventricular muscle^{11–13}. These developments could serve as a role model for SD modeling in migraine and stroke research, and inform us in particular which questions require what type of model.

Two types of models for SD

Computational models for SD conceptually consist of two parts: one part that models microscopic processes, i.e. the interactions within a single neurovascular unit leading to local failure of homeostasis and breakdown of the ion gradients, and a second part that describes the interactions throughout the tissue, usually through diffusion, leading to the macroscopic propagation of the homeostatic disturbance (Figure 2). The latter is usually described by relatively simple expressions for diffusion. The microscopic interactions, however, are much more complex. For example, the concentration dynamics of potassium depend on the neuronal membrane voltage dynamics, buffering by glial cells and diffusion to the blood vessels. These microscopic processes can be modeled with either detailed biophysical models, or by more abstract models of so-called activator–inhibitor type.

The detailed biophysical models are suitable to inves-

^{a)}Corresponding author:

Bas-Jan Zandt, PhD

Email: Bas-Jan.Zandt@biomed.uib.no

Department of Biomedicine

Postboks 7800

5020 Bergen

Norway

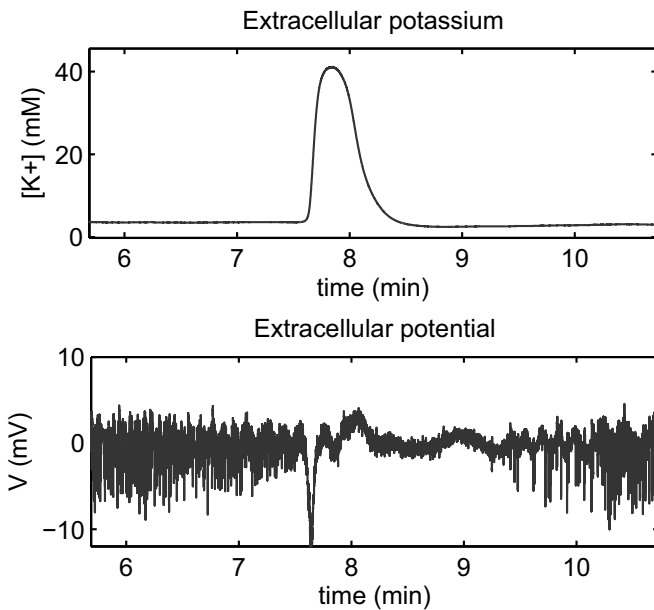


FIG. 1. Disturbed ion concentrations and suppression of neuronal electrical activity. Extracellular potassium concentration (upper panel) and extracellular potential (lower panel) during SD at a fixed position (in vivo rat cortex). Sudden release of neuronal K^+ into the extracellular space is observed at $t = 7.7$ min. Redistribution of ions (K^+ , Na^+ , Cl^- and Ca^{++}), between the intra- and extracellular space results in temporary neuronal dysfunction and cessation of extracellular electrical activity. In these normoxic conditions, recovery of $[K^+]$ (after 1 min) and electrical activity (after 2-3 min) is relatively fast. The disturbance was observed to be traveling over the cortex at several mm/min. (Backes, Feuerstein, Ima, Zandt and Graf, unpublished data)

tigate microscopic processes: the time-course of ions, transmitters, channels and pumps, and their contribution to SD. Abstract activator-inhibitor models are better suited to understand macroscopic behavior: the propagation and pattern formation of SD waves. However, many important questions include both aspects: How can non-invasive stimulation break up an SD wave? What is the neural correlate of EEG and fMRI signals recorded during peri-infarct depolarizations? Which combination of channel blockers efficiently blocks SD propagation? What are critical differences between human patients and animal models? These questions show the need for combining the two approaches, and linking parameters of abstract models to the behavior of biophysical models.

Outline

This review discusses the two main types of models used to study SD, their advantages and disadvantages, and the recent advances in techniques to link them. We start however, by discussing the basic biophysics and physiology of SD that is used to construct these mod-

els.

II. PHYSIOLOGY OF SD

The reviews of Somjen¹⁴ and Pietrobon and Moskowitz¹⁵ discuss the phenomenology, physiology and pharmacology of SD in great detail. Here we focus on the basic physiological and biophysical concepts important for computational modeling of SD.

Experimentally, SD can be induced by various stimuli, including ischemia, intense electrical stimulation, mechanical damage (needle prick) or application of K^+ or glutamate. These are all stimuli that directly or indirectly increase neuronal excitability or depolarize neuronal membranes. Similar to an action potential, once triggered, SD propagates in an all or none fashion, independent of the stimulus type or intensity.

Four hypotheses exist to explain the propagation of SD. The potassium and glutamate hypotheses state that SD propagates through diffusion of extracellular potassium or glutamate respectively. The neuronal gap junction hypothesis states that SD propagates by opening of neuronal gap junctions, while the glial hypothesis assumes that SD is caused by transmission through glial gap junctions. Evidence seems to favor the potassium hypothesis¹⁵, although neither of the hypotheses can fully explain the experimental observations, and propagation is probably realized by a combination of these mechanisms¹⁴. In line with most modeling work on SD, we will also focus on release and diffusion of extracellular potassium and glutamate, and do not discuss propagation via neuronal or glial gap junctions.

First, we will discuss how extracellular potassium and glutamate stimulate their own release when homeostasis mechanisms are overchallenged and how this leads to sustained neuronal depolarization. Then, diffusion to neighboring tissue of the released substances is discussed and how movement of ions induces extracellular voltage gradients. Subsequently we elaborate on the recovery processes that enable restoration of the ion gradients and electrical activity and discuss the role of cell swelling and synapses in SD.

A. Homeostasis of the neurovascular unit fails during SD

Proper neuronal functioning relies on a steady supply of energy in the form of glucose and oxygen from the blood, as well as support from glia cells maintaining homeostasis of the extracellular composition. The neurovascular unit is a useful theoretical concept for describing (patho)physiology of neural metabolism. This unit consists of neuronal and glial intracellular space (ICS), the extracellular space (ECS) and a capillary supplying blood flow. The metabolic and homeostatic processes in such a unit determine largely how neural tissue reacts

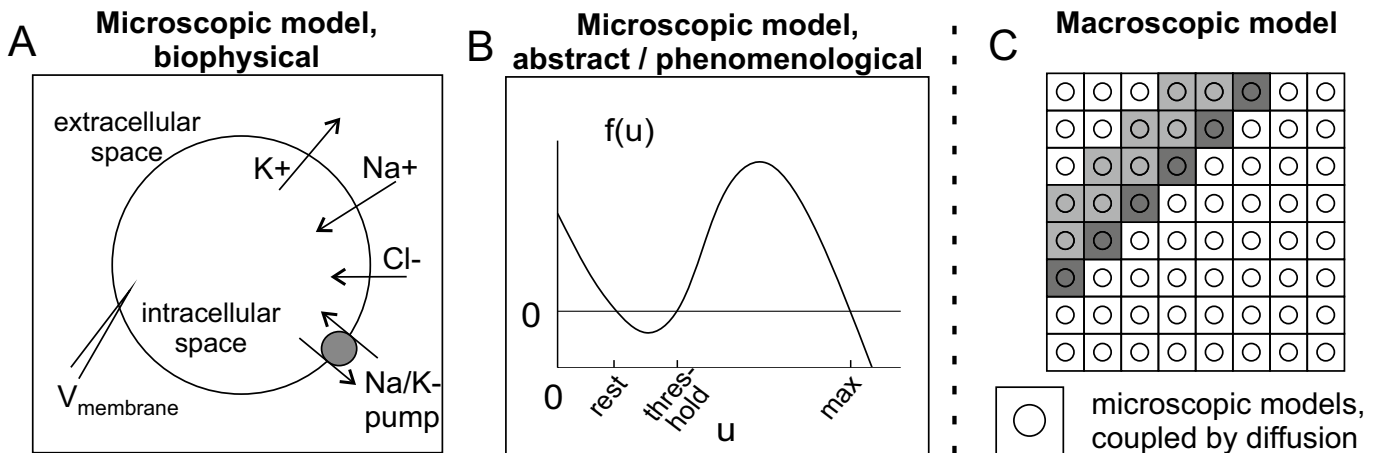


FIG. 2. Modeling of SD. The microscopic interactions within the tissue (the “reaction part”) can be modeled with a biophysical model, describing the ionic currents and release of neurotransmitters (panel A). Alternatively, a phenomenological or abstract model can be used, in which only one or two effective variables are considered that represent activation and recovery (panel B). Using these models, a plane or grid can be constructed to investigate SD propagation (Panel C).

to ischemic and homeostatic insults such as SD and ischemia.

Extracellular potassium and glutamate concentrations are tightly regulated in the brain. During rest, potassium ions leak from neurons, while action potentials and synaptic input increase this efflux even more. An estimated 70% of the energy produced in the brain is consumed by neuronal Na/K-pumps and other ion transporters, in order to maintain physiological ion gradients over the neuronal membranes¹⁸. High extracellular potassium concentrations strongly increase neuronal excitability and hence glia cells rapidly take up excess amounts of potassium from the ECS. Furthermore, glia cells absorb glutamate released from excitatory synapses. Figure 3A shows the main processes involved in the homeostasis of extracellular potassium and glutamate.

Rapid buffering of these two substances is critical, since they excite neurons and thereby stimulate their own release. This results in a positive feedback loop. Indeed, when a stimulus increases their concentration beyond a certain threshold, neuronal and glial transporters cannot cope with the efflux (Figure 3B). This results in massive release of potassium and glutamate and leveling of the ion gradients, which disables the generation of action potentials.

B. Sustained depolarization results from shifts in ion concentrations

Each ionic species has a Nernst, or reversal, potential E that drives the ionic current through the neuronal membrane. This electrical potential results from the concentration gradients across the semi-permeable membrane. Importantly, this voltage is determined by the intra- and

extracellular ion concentrations:

$$E = \frac{RT}{zF} \ln \frac{C_{in}}{C_{out}}, \quad (1)$$

where F and R are the Faraday and universal gas constant, T the absolute temperature, and z the valence of the ion species. Although more accurate expressions, such as the Goldman-Hodgkin-Katz (GHK) equations, have been derived¹⁹, the Ohmic currents in the Hodgkin-Huxley (HH) equations suffice to qualitatively explain the neuronal electrophysiology during SD²⁰. These show the resting membrane voltage is determined by the average Nernst potential, weighted by the respective ionic conductances g :

$$V_r = \frac{g_{Na}E_{Na} + g_K E_K + g_{Cl}E_{Cl}}{g_{Na} + g_K + g_{Cl}}. \quad (2)$$

Hence, the neuronal membrane can be depolarized in two ways: changes in conductances and changes in Nernst potentials. An increased conductance of an outward current occurs for example during action potentials. During the upstroke of the action potential, the sudden opening of sodium channels temporarily generates an outward current that is not balanced by inward currents. This results in a fast (submillisecond) depolarization of the membrane voltage. The surplus of charge entering the cell resides in a very small region near the cell membrane²¹, thus preserving electroneutrality in the solute. During SD, the glutamate level in the ECS rises¹⁴, increasing the sodium conductance. This may induce the initial depolarization of neurons, according to the glutamate hypothesis.

In contrast, the sustained depolarization and slow membrane voltage dynamics observed during SD are due to a more gradual (seconds) change of the resting membrane voltage, mediated by changing intra- and extracellular ion concentrations (equations 1 and 2). Large numbers of ions flow across the membrane during SD,

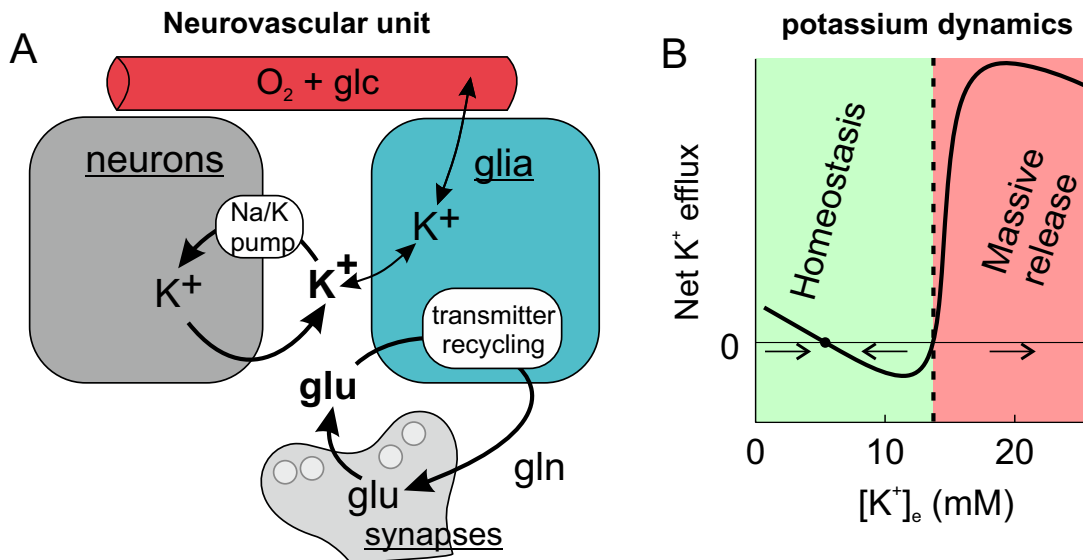


FIG. 3. Homeostasis of extracellular potassium and glutamate in the neurovascular unit. Panel A schematically shows the main release and uptake pathways. Potassium leaking from the neurons and released during action potentials is pumped back by the Na/K-pump. Synaptically released glutamate (glu) is taken up by glia cells, and returned in the form of glutamine (gln). In addition, glia can rapidly buffer K^+ , distribute it over the glial syncytium and transport it to the blood stream. A constant supply of oxygen and glucose from the blood is necessary to fuel these processes. Adapted from¹⁶. Panel B shows a sketch of the dynamics of extracellular potassium. Up to a threshold (dashed line) of typically 8-20 mM, elevated extracellular potassium increases its own removal from the extracellular space by stimulating Na/K-pumps and glial uptake. This restores the concentration to the physiological set point (black dot). Above threshold (dashed line), potassium is released into the extracellular space faster than its removal due to stimulation of neuronal action potential generation. Based on¹⁷. The dynamics of extracellular glutamate show a similar threshold (not shown).

TABLE I. Typical neuronal ion concentrations²² and corresponding Nernst potentials.

	Intracellular (mM)	Extracellular (mM)	Nernst Potential (mV)
Na^+	13	140	60
K^+	140	4	-95
Cl^-	4	120	-90

and these tend to equilibrate the concentrations of the ICS with the ECS. The membrane voltage and ion concentrations shift towards the Donnan equilibrium¹⁴. In this equilibrium the ion gradients and membrane voltage are close to zero, but do not completely vanish due to large charged molecules in the ICS that cannot cross the neuronal membrane. The currents generated by ion pumps and transporters, as well as the slow Cl^- dynamics, keep the cell from fully reaching the Donnan equilibrium. We will therefore refer to this depolarized state as the near-Donnan state, to distinguish it from “ordinary”, conductance mediated, depolarization.

Extracellular potassium plays an important role in the triggering and propagation of SD. Of the main ionic species in the ECS and ICS, i.e. Na^+ , K^+ and Cl^- , extracellular potassium influences the resting membrane potential most. Its concentration is relatively low (table I) and the extracellular space relatively small. Hence, transmembrane fluxes can elevate this concentration rel-

atively rapidly. In addition, the potassium conductance is relatively large such that E_{rest} is close to E_K .

Note that, since the ECS and ICS need to remain electroneutral, and the capacitance of the membrane is limited, no net electrical current can flow across the membrane on the time scales of seconds or longer. Therefore, changes in ion concentrations and sustained depolarization cannot result from a single ionic current, but is rather mediated by a set of opposing currents. The necessity for balanced, opposing currents should be kept in mind when, for example, interpreting measurements in which specific currents are blocked to investigate which currents play a role in SD. For example, reducing the potassium conductance by partly blocking K^+ channels hardly lowers potassium efflux, since this is typically limited by the sodium influx. Instead, this depolarizes the resting membrane voltage²³ and when this depolarization is large enough, voltage gated sodium channels open, allowing for a rapid efflux of potassium and subsequent depolarization^{24,25}.

C. Diffusion of potassium and glutamate can propagate SD

After potassium and glutamate are released locally, they diffuse to neighboring tissue, and can thereby propagate an SD (see Section III). During propagation, the

front of the SD wave extends over several 100 μm 's in the longitudinal direction, and hence SD propagation is a smooth process, rather than a chain reaction from neuron to neuron²⁶.

While diffusion from a fixed source becomes progressively slower over longer distances, an RD process (SD) propagates at a steady velocity by recruiting medium (tissue) at the front of the wave as new source. For an idealized case, the velocity is given as²⁷:

$$v = \sqrt{\frac{RD_{\text{eff}}}{\Delta C}}, \quad (3)$$

where R is the rate at which neurons expulse potassium or glutamate, D_{eff} the effective diffusion constant and ΔC the concentration threshold above which neurons start expulsing this substance.

Tortuosity

The diffusion constants in water are $2.1 \times 10^{-9} \text{m}^2/\text{s}$ and $0.76 \times 10^{-9} \text{m}^2/\text{s}$ for K^+ and glutamate, respectively (at 25°C)^{28,29}. However, the large cell density in neural tissue hinders diffusion, and the effective diffusion coefficient D_{eff} in ECS is typically a factor 2.5 lower than the free diffusion constant D . This is denoted by the tortuosity λ , historically defined as $\lambda^2 = D/D_{\text{eff}}$. Typically $\lambda = 1.6$ for ECS^{30,31}. Syková and Nicholson³² extensively review the physiology of diffusion in the extracellular space.

Electro-diffusion

Often overlooked, however, is that in contrast to electrically neutral particles, potassium and glutamate are charged substances that cannot diffuse freely. A displacement of e.g. K^+ ions induces a voltage gradient in the tissue. The resulting electrical force (drift) counteracts the diffusion. Hence, the amount of K^+ that diffuses will be substantial only when there is counter movement of cations or co-movement of anions. This phenomenon is referred to as electro-diffusion. The voltage induced by the diffusion of ions creates a liquid junction potential and can be calculated with the Goldman-Hodgkin-Katz (GHK) expressions^{19,33}. (For expressions correctly taking the transmembrane currents into account see³⁴.) The main contributors in ECS are K^+ , Na^+ and Cl^- . Considering only these species, the extracellular voltage due to diffusion between two points in close proximity is calculated as:

$$\Delta V = \frac{RT}{F} \ln \left(\frac{D_{\text{K}}[\text{K}^+]_1 + D_{\text{Na}}[\text{Na}^+]_1 + D_{\text{Cl}}[\text{Cl}^-]_2}{D_{\text{K}}[\text{K}^+]_2 + D_{\text{Na}}[\text{Na}^+]_2 + D_{\text{Cl}}[\text{Cl}^-]_1} \right), \quad (4)$$

where the subscripts 1 and 2 denotes the concentrations at the two points in the extracellular space. The extra-

cellular currents are calculated for each ion species as³⁵:

$$\vec{I} = \underbrace{-zF \frac{D}{\lambda^2} \vec{\nabla} C}_{\text{diffusion}} + \underbrace{\frac{z^2 F^2}{RT} \frac{D}{\lambda^2} C \vec{\nabla} V}_{\text{drift}}, \quad (5)$$

where C denotes the extracellular concentration of the ionic species and z its valency. This expression was used by Qian and Sejnowski³⁶ to adapt the cable equations for non-homogeneous ion concentrations in the ECS.

Using a numerical model including electro-diffusion in the ECS, Almeida et al.³⁵ calculated the extracellular voltage during SD that arises from diffusion of K^+ , Na^+ and Cl^- to be approximately -14 mV, which is in agreement with experimental observations (cf. Figure I).

In most modeling studies of SD, extracellular potassium and glutamate are assumed to follow ordinary diffusion laws rather than those of electro-diffusion. This is a reasonable approximation, as long as a composite diffusion coefficient is used³⁷, which takes co- and counter-diffusion of the ions in the ECS into account.

D. Recovery mechanisms

Under normoxic conditions, ion concentrations start to recover typically a minute after SD onset. Electrical activity returns after a few minutes. Several mechanisms contribute to the tissue's recovery. A critical factor is that the Na/K-pump has to overcome the potassium efflux. Therefore, mechanisms are necessary that reduce potassium efflux, stimulate pump activity, and support this activity by a sufficient supply of energy.

Na/K-pump and glial potassium removal

To recover neuronal function, physiological ion concentrations in the ECS and ICS need to be restored after SD. Both increased intracellular sodium and extracellular potassium levels stimulate the Na/K-pump³⁸⁻⁴⁰. This is insufficient to counteract the potassium efflux, however. In fact, this insufficiency was what instigated the depolarization process in the first place. Therefore, a critical step in the recovery process is the repolarization of the neuronal membrane voltage. This closes the voltage gated channels, greatly diminishing the potassium efflux, thereby allowing the pump to restore the physiological concentrations. The repolarization is effected by glial buffering of extracellular potassium from the extracellular space^{24,41}, lowering E_{K} , and thereby the membrane voltage (equations 1 and 2).

Depending on the type of cell and brain area, the transmembrane voltage can be near 0 mV during SD, at which transient and NMDA-gated sodium channels are inactivated. Therefore, a yet unidentified conductance is argued to be activated in these cells during SD⁴². The sodium current through this conductance delays the recovery process.

Functional hyperemia

The increased activity of the Na/K-pumps must be met with an increased blood flow, i.e. functional hyperemia, supplying additional oxygen and glucose to the tissue. The signaling pathways for vasodilation following increased neural activity⁴³ are mediated by astrocytes^{44,45}, and include amongst others Ca^{2+} , K^+ , adenosine, nitric oxide and arachidonic acid⁴⁶. These pathways mainly sense neuronal activity, rather than oxygen or glucose availability⁴⁷. For large disturbances, such as SD, the vessel response is strongly non-linear. While moderate increases of extracellular potassium cause vasodilation, stronger increases induce vasoconstriction⁴⁸ (and references therein). The neurovascular response to SD typically shows a triphasic response (constriction, dilation, followed by a prolonged, slight constriction), but differs greatly over species and conditions, ranging from pure constriction to pure dilation⁴⁹.

Neurovascular coupling is a subject of active investigation, mostly in the light of the blood-oxygen-level-dependent (BOLD) response recorded by functional MRI (fMRI)^{50,51}. When investigating (hypoxic) SD, it should be kept in mind that the normal neurovascular response is altered by effects induced by SD and hypoxia, such as changes in pH^{14,52,53}.

Synaptic failure

SD induces temporary synaptic failure. This failure reduces synaptic currents and suppresses electrical activity, thereby reducing the neuronal energetic needs. The cause of the failure is presynaptic, evidenced by the facts that electrical activity remains suppressed for several minutes after repolarization and that neurons do generate action potentials upon application of glutamate during this period⁵⁴. Synaptic failure is induced by high extracellular levels of adenosine, a break-down product of ATP, preventing the vesicular release of glutamate. Adenosine levels may increase as a result of increased ATP consumption, as well as from the release of ATP in the ECS^{54,55}.

E. Role of cell swelling and synaptic interactions in SD

Cell swelling

Neurons regulate their volume and intracellular osmotic values with a variety of ion transporters and exchangers, aided by stretch sensitive ion channels⁵⁶. Changes in ion concentrations during SD alter the osmolalities of the ECS and ICS. This induces osmotic influx of water and consequent cell swelling, thereby equalizing the osmolalities. Cell membranes are highly permeable to water and do not sustain significant osmotic pressures, such that water influx must fully equalize the osmotic values of the ICS and ECS⁵⁷. Note that exchange of Na^+

and K^+ does not change osmotic values. Hence transmembrane fluxes of anions or divalent cations, e.g. Cl^- or Ca^{2+} , are necessary for cell swelling to occur⁵⁸.

Most biophysical models of SD, discussed in section III A, calculate the evolution of the ion concentrations. These models can therefore naturally be extended with cell swelling. With the notable exception of the model by Shapiro⁵⁹, most computational work shows that cell swelling mainly follows the dynamics of the ion concentrations during SD, rather than having a fundamental role in the initiation and propagation.

Synapses

Synaptic transmission is not necessary for SD propagation¹⁴, and perhaps therefore, current computational models for SD are restricted to neurons without synaptic input. This is certainly realistic in hypoxic conditions, where synapses quickly fail⁶⁰. In normoxic conditions, however, synapses function normally at the onset of SD. Therefore, neuronal activity is determined by network dynamics and inhibitory feedback, rather than by single cell dynamics alone. Since inhibitory neurons are also excited by elevated extracellular concentrations of potassium and glutamate, the corresponding increase of overall firing rates, and hence release of K^+ and glutamate, may be less drastic than for isolated cells. In correspondence, blocking (inhibitory) GABA receptors has been shown to induce SD^{61,62}. Furthermore, prodromals, intense neuronal firing before depolarization, may alter the neuronal activity around the front of the wave through long range synaptic connections, influencing SD propagation.

So far, little theoretical work has been performed on the influence of network activity, local inhibition and long range connections on SD propagation and initiation.

III. MODELING SPREADING DEPRESSION

Broadly speaking, two types of computational/mathematical models for SD and peri-infarct depolarizations can be distinguished.⁶³

On the one hand, there are bottom-up, biophysical models, whose variables describe physiological quantities. These models consist of sets of differential equations describing the neuronal membrane voltage dynamics, ion and neurotransmitter fluxes and concentrations, and activity of homeostasis mechanisms. These models extend the traditional conductance based, i.e., HH-type, models with dynamics of the concentrations of ions and neurotransmitters in the ECS and ICS. They typically contain several equations and many parameter values for conductances and pump rates.

On the other hand, there are more phenomenological or abstract models. These typically describe only the dynamics of one variable, e.g. the extracellular potassium

concentration or the general level of excitation. Some models then add a second variable that summarizes the processes enabling recovery.

A bottom-up biophysical model is necessary if one is interested in the profile of various physiological quantities that play a role in the spread of SD. Since the equations represent clear biophysical interactions, the mode of action of e.g. a neuroprotective agent, channel mutation or stimulation can be included in such a model in a straightforward way. However, analyzing the dynamics of such a detailed model is complicated, and the investigator is left with performing experiments with the model in a similar manner as with real world tissue.

In contrast to the questions on the biophysics, there are clinical questions that concern the general propagation of SD. For example, the spread of SD waves in a full-scale migraine attack with aura determines the sequence of various symptoms⁶⁴. The SD pattern spans over tens of centimeters in the cortex and can last hours. In this case, there clearly is a need for a model of SD with simplified dynamics that effectively describes large and sustained patterns in 2D, without the need to follow all physiological quantities on a cellular level.

While such a more phenomenological or abstract model allows for mathematical analysis, revealing the basic properties of SD initiation and propagation, it is no longer possible to explicitly include the action of drugs or channel mutations in the model. Explicitly linking detailed and phenomenological models, i.e., deriving simplified models from more detailed ones, allows to investigate how such conditions affect the parameters of a simplified model.

A. Conductance based models with dynamic ion concentrations

Several microscopic models have been constructed to describe the ionic fluxes/currents and corresponding dynamics of the concentrations in the intra- and extracellular spaces (Figure 2A). Some of these models were specifically designed to describe neuronal depolarization and spreading depression, while others were designed to explain bursting and epileptiform activity induced by ion concentration dynamics. The latter can be used to investigate neuronal depolarization as well. The review of Miura et al.⁶⁵ discusses the most prominently used models for SD in more detail, as well as the differences between these models and their specific findings. Here we will focus on the general form and use of these models.

Microscopic, single unit models

The simplest current based models consider an extracellular space and a neuron modeled as a single (somatic) compartment^{25,66–68}. This compartment has a neuronal membrane with leak currents and voltage gated Na and

K-channels as in the HH model, and a Na/K-pump. The ion concentration dynamics in the intracellular compartment are driven by the fluxes of ions through the neuronal membrane, i.e., the leak, gated and pump currents. The concentrations in the extracellular space are additionally regulated by homeostatic mechanisms such as diffusion to the blood and glial potassium buffering. The original HH model, with only two gated channels, was shown to be sufficient to explain the various types of membrane voltage dynamics observed during depolarization of rat pyramidal cells in vitro²⁷.

More detailed models have been constructed that include one or multiple dendritic compartments and/or additional ion channels^{24,42,69–75}. These more elaborate models allow for better quantitative agreement with experimental data, and investigation of the contribution of specific ion channels to SD vulnerability and seizures.

The observed dynamics of these models are qualitatively all similar. In general, depolarization can be induced in these models by application of extracellular potassium or glutamate, release of potassium from intense stimulation or temporary halt of the Na/K-pump. This results in an initial moderate depolarization of the resting membrane voltage. If this depolarization is large enough, voltage gated sodium channels open, greatly increasing potassium efflux, leading to sustained depolarization.

These single unit models can be used to investigate what mechanisms trigger or prevent depolarization locally in the tissue, as well as the mechanisms for recovery. The more simple models allow for bifurcation analysis of the local ion dynamics, which can identify parameters, e.g. pump strengths or potassium inflow, that cause critical transitions between the physiological stable state, cycles of depolarization and recovery, or permanent depolarization^{20,41,66}.

Models with one- and two-dimensional space

In order to investigate the actual propagation of SD, the above discussed microscopic models must be extended with a spatial component and extracellular diffusion (Figure 2C)^{26,59,76,77}, or electro-diffusion^{59,78}.

Most models that investigate SD have at most two dimensions, since the cortex is basically a folded, two-dimensional, sheet. However, investigating propagation analytically is much simpler in one dimension. Therefore, models are often reduced to one dimension, by arguing that the wave front of SD is relatively straight. To increase computational speed and lower complexity further, some models neglect the dynamics of the voltage gated channels and thereby remove neuronal action potentials from the model^{76,77,79}. This is justified because this simplification does not qualitatively alter the ion concentration dynamics during SD, although it may quantitatively alter, for example, the critical stimulus strength for inducing depolarization.

In addition to electro-diffusion, Shapiro⁵⁹ included gap junctions and cell swelling in his model. In support of the gap junction hypothesis, he finds that both the current through the gap junctions as well as the concentration increase due to cell swelling is necessary for SD propagation, while extracellular diffusion does not significantly contribute to SD propagation. He shows that this effect is robust for variation in the parameters. However, most other models produce propagating SD waves without gap junctions or cell swelling. A reason for this may be differences in the conductance parameters, which can change over orders of magnitude between cell types and brain areas. However, the exact reasons for the different findings are not clear, since these models are hard to analyze without further simplification. This illustrates the main drawback of such very detailed models.

Finally we remark that all current models used to investigate SD propagation are essentially isolated cell models, i.e., they do not include the effects of synaptic interactions and network dynamics on the ion concentration dynamics. Ullah et al.⁸⁰ model the activity of a network of excitatory pyramidal cells and inhibitory interneurons and the corresponding ion concentration dynamics, although they do not explicitly consider SD. Their model would be suitable for investigating how inhibitory feedback and network dynamics affect triggering and propagation of SD, an issue on which research has been lacking so far.

B. RD models of activator–inhibitor type

There is more literature on very basic reaction–diffusion (RD) models in SD than we can cover in detail in this review^{35,76,81,82}. We focus on SD pattern formation in three essential steps from (i) modeling propagation of the wave front, to (ii) modeling propagation and recovery (a pulse) to (iii) modeling localized patterns.

Wave front propagation

Grafstein⁸³ originally proposed the potassium hypothesis and—based on a suggestion by Hodgkin that included mathematical analysis from Huxley—she was the first to present an RD model of extracellular potassium concentration ($[K^+]_e$) dynamics in neural tissue that supports her experimental observations and leads to roughly the correct speed of SD⁸⁴.

Grafstein considered the effects of potassium release by the cells and potassium removal by the blood flow. The RD model describes the dynamics of the extracellular potassium concentration, $[K^+]_e$ or simply u , with a rate function $f(u)$ that is a third order polynomial with roots $f(u) \equiv 0$ chosen at resting level concentration, threshold concentration (later called ceiling level by Heinemann and Lux⁸⁵) and maximum concentration (cf. Figure 3B).

Together with diffusion this yields:

$$\frac{\partial u}{\partial t} = f(u) + D_u \nabla^2 u. \quad (6)$$

Since recovery is not modeled, $[K^+]_e$ is locally bistable and can be resting at either the physiological resting level or the maximum concentration (pathological state). The variable u , the $[K^+]_e$, is also called an *activator*, because it activates a positive feedback loop when above a certain threshold. A stimulus, i.e., local application of potassium, can increase $[K^+]_e$ above threshold, releasing additional K^+ . A sufficiently large stimulus⁸⁶ triggers a traveling wave front, i.e., an SD, that eventually recruits all the medium in its state.

Including recovery - pulse propagation

Reggia and Montgomery^{87,88} have built the first computational model that aimed at reproducing the typical zigzag of a fortification pattern experienced as visual field defects during migraine with aura,^{89,90}. One part of this model is an RD model for SD based on potassium dynamics, similar to that of Grafstein and Hodgkin. However, it introduced two new features.

First their model includes a second variable describing the recovery process that drives the maximum $[K^+]_e$ back to the physiological resting level. For uniformity we refer to this recovery variable as v (r in the original papers). This was not the first such model with recovery, see e.g.^{76,81}, but we emphasize it here, because it directly links with earlier and later models discussed in the previous and the next section.

The recovery process is modeled phenomenologically as an additional removal of potassium. This recovery process, described by v , is slowly activated when $[K^+]_e$ increases:

$$\frac{\partial u}{\partial t} = f(u) - v + D_u \nabla^2 u, \quad (7)$$

$$\frac{\partial v}{\partial t} = \varepsilon(c_1 u - v). \quad (8)$$

c_1 determines the magnitude and ε the activation time of the recovery, which is on a slower time scale (minutes) than the potassium concentration dynamics. When v becomes sufficiently large, $[K^+]_e$ recovers to the physiological resting level. After this recovery, v remains heightened for some time, leading to absolute and relative refractory periods for inducing a second SD.

v is also called an *inhibitor* as it inhibits the release of potassium ions (the *activator*). RD models of activator–inhibitor type account for many important types of pattern formation, such as spiral-shaped waves. There is a vast body of literature of activator–inhibitor models on chemical waves and patterns⁹¹, which directly applies to propagation of SD.

Global inhibition - localized patterns

The models discussed so far, cannot account for the observation, from noninvasive imaging and reported visual field defects, that SD waves in migraine aura may propagate as a spatially localized pattern within the two-dimensional (2D) cortical sheet, rather than engulfing the entire cortex^{92–94}. This localization in 2D requires a third mechanism (the first two being the activator for front propagation and the inhibitor for pulse propagation in 1D, which can only explain engulfing ring pulses in 2D).

In fact, another major new feature in the model by Reggia et al.^{87,88} is going half way the third and last step from fronts to pulses to localized patterns. Their RD model is coupled to a neural network, used to predict the visual field defects during migraine with aura. In brief, the mean firing rate of neurons at time t in each “cell” (population of neurons) is represented by an activation level $a(t)$. They phenomenologically let $[K^+]_e$ modulate this activation level, such that subthreshold increases of $[K^+]_e$ stimulated activity, while superthreshold concentrations depressed activity. Furthermore, the neural network has lateral synaptic connections, such that cortical cells excite nearby cells and inhibit cells more distant (“Mexican hat” connectivity).

This is novel, because the model incorporates as spatial lateral coupling not only local diffusion, but also synaptic long-range connections. However, the neural network dynamics were not fed back to the actual RD model (Equation (8)) and hence it remains an open question how the local and long range synaptic connections in the neural network influence the SD dynamics (see Section II E). Nevertheless, long-range coupling is an essential mechanism for the emergence of localized patterns.

Dahlem and Isele⁹⁵ proposed that long-range coupling is established by the neuroprotective effect of increased blood flow induced by SD (Section II D). In their model this increase in blood flow was assumed to be global, and its effect was phenomenologically incorporated as an inhibition process throughout the entire tissue. This global inhibitory feedback limits the spread of SD to traveling, localized spots on the (two-dimensional) cortical sheet, protecting it from a larger—possibly engulfing—recruitment into this pathological state.

According to the model, SD waves are initially spreading out radially. In a fraction of simulated SD attacks, the circular wave breaks open to a segment after not later than a few minutes and then propagates further in one direction only. The arc length (width) of the SD front line, was estimated using this model to be between a few millimeters up to several centimeters⁹⁵. This is in accordance with the precise reports of visual symptoms of his own aura by Lashley⁸⁹, see Fig. 4 left.

Furthermore, Dahlem and Isele⁹⁵ investigated the shape and form of SD patterns in single attacks, as well as their duration. They studied how these properties change for different degrees of cortical susceptibility to

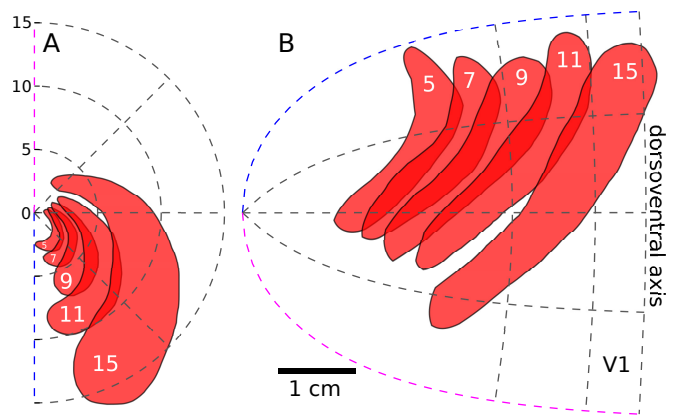


FIG. 4. Five snapshots of a traveling visual migraine aura symptoms. From the precise reports of visual symptoms by Lashley⁸⁹ of his own aura, for this particular example the width of the wave front of 4 cm was estimated by retinotopically mapping the symptoms to the primary visual cortex⁹³.

SD and claimed these emergent macroscopic properties can be linked to the prevalence of the major migraine subtypes, i.e., migraine with and without aura. They hypothesize that migraine pain induced by inflammation is only initiated if a large surface area is simultaneously covered by the SD pattern, and the aura symptoms, on the other side, can only be diagnosed if SD stays long enough (>5 min) in the cortex. The analysis revealed that the severity of pain and aura duration are then to some degree anti-correlated and, furthermore, cortices being less susceptibility to SD can exhibit still short-lasting but significantly large SD patterns that may underlay the concept of “silent aura”, i.e., migraine without aura but pain caused by SD⁹⁶.

The Dahlem model was inspired by a previous RD model⁹⁷ that shows propagation of spots in 2D can be described by global inhibition. Such propagating spots were observed in semiconductor material, gas discharge phenomena, and chemical systems. Due to the global inhibition this is not a classical RD model. However, it closely resembles a classical RD model with one activator u and two inhibitors v and w ^{98,99}:

$$\frac{\partial u}{\partial t} = f(u) - v - w + D_u \nabla^2 u, \quad (9)$$

$$\frac{\partial v}{\partial t} = \varepsilon (c_1 u - v), \quad (10)$$

$$\frac{\partial w}{\partial t} = \theta (c_2 u - w) + D_w \nabla^2 w. \quad (11)$$

When the diffusion constant D_w is set very large, w acts as global inhibitory feedback (see figure 5).

The physiological substrate of these three lumped variables will be further elaborated on in the next section. As such, these RD models are merely top-level descriptions that still lack a solid bottom-up derivation from the positive feedback loop in potassium and other ion con-

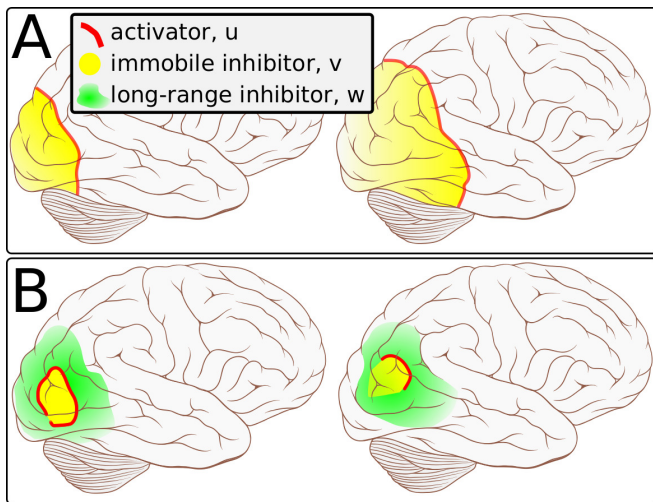


FIG. 5. **Spatio-temporal development of SD.** (A) Classical pattern formation paradigm, SD starting from an ictogenic focus in all directions and engulfing in a full-scale attack all of posterior cortex. (B) In the new paradigm, SD is a localized pattern that, when it breaks away from the ictogenic focus, it necessarily needs to break open and assumes the shape of a wave segment. Colors mark high activity (or concentration) of activator and inhibitors.

centrations, electrical activity and homeostatic recovery mechanisms.

C. Linking generic RD models to conductance based models

Model reduction

The ad hoc description in Sect. IIIB leaves important questions unanswered: What exactly are these lump variables u , v , and w ? Which quantities have been lumped together and how? Is a polynomial rate function a generic description? To answer these, one might think of adding more and more details to the top-level description started by Grafstein⁸³ and eventually reach a description on the level of conductance-based models with dynamic ion concentrations, but the reverse way is more natural, a bottom-up approach starting from a conductance-based model with dynamic ion concentrations.

The first of two key steps is to reduce the conductance-based models. These models can contain several dozens of dynamical variables. A reduction makes them tractable for a detailed bifurcation analysis using a continuation software package, like AUTO¹⁰⁰ that further leads to generic RD models with lump variables once the bifurcations have been identified.

For example, several reduction techniques such as adiabatic elimination, synchronization, mass conservation, and electroneutrality have been used to reduce a conductance based model of SD to only four dynamic vari-

ables, while this model still retains adequate biophysical realism²⁰.

Towards identifying u , v , and w

To further discuss the details of the activator u and two yet unknown inhibitors v and w , it is insightful to divide the reduced conductance-based model with dynamic ion concentrations into two parts: the intracellular and extracellular compartment with the separating membrane containing the voltage-gated channels (the cellular system) and some ion buffer (the reservoir).

As discussed, the activator dynamics without an inhibitor (recovery mechanism) (Equation (6)) lead to a bistability. In a conductance based model, the isolated cellular system without coupling to a reservoir was also found to be bistable²⁰. The bistability is seen in extracellular $[K^+]_e$ (Figure 6), but it is best characterized by the full state of the cellular system. One stable state is the physiological resting state, far from thermodynamic equilibrium. The other state is the depolarized, near-Donnan state, close to the thermodynamic equilibrium of a semipermeable membrane (section IIB). These two states are separated by an unstable equilibrium.

In this closed system, the activator u can directly be identified as the amalgamation of the variables that form the bistability, notably the extracellular potassium concentration.

Following this ansatz further, the local inhibitor v is identified as the potassium ion gain via external reservoirs, i.e., blood and glia cells. A loss (negative gain) of potassium ions both renders the near-Donnan state unstable, causing the system to recover, as well as increases the threshold for SD in the physiological resting state. This reservoir coupling takes place on the slowest time scale of the system⁴¹, and hence the potassium ion gain can also be considered as a bifurcation parameter (Fig. 6). Note that the ion gain as a bifurcation parameter is qualitatively different from the ion bath concentration in the reservoir, which is often used as a bifurcation parameter^{66,71,72,74}. In fact, the essential importance of the potassium ion gain as a slow inhibitor and hence useful bifurcation parameter was not realized in earlier studies⁴¹.

The long-range inhibitor w , may be related to neuronal activation, i.e., action potentials, for example through changes in long-range synaptic activity. Alternatively, it may be related to global blood flow regulation. However, w cannot be identified from a model of a single neurovascular unit, since it represents an interaction that is essentially non-local.

Bifurcation analysis and generic models

The second key step is to link this reduced conductance based model to a generic RD model with lump variables

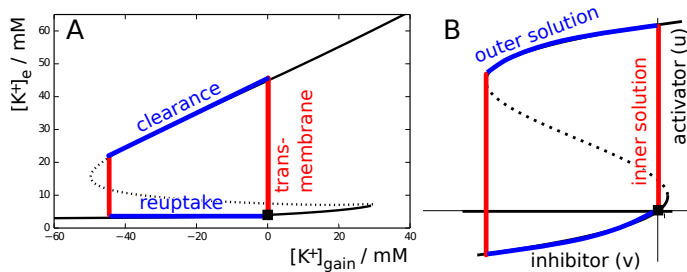


FIG. 6. (A) Bifurcation diagram of HH model with dynamic ion concentrations using mols of potassium ions gained from a reservoir as a bifurcation parameter⁴¹. Note that this parameter is given in terms of a concentration with the reference volume being that of the extracellular space. SD is marked as a counter-clockwise cyclic process starting from the physiological state (black square). Vertical subprocesses (red) occur at constant ion content, i.e., these are the fast pure transmembrane ion fluxes. Subprocesses with a horizontal component (blue) involve potassium ion clearance (right to left) or ion reuptake (left to right). The dotted and solid black line is the unstable and stable part, respectively, of the fixed point branch. The dotted line marks a threshold. (B) Phase space of a generic (i.e., polynomial) model described in Eqs. (7)-(8). Subsections of an excitation cycle can be obtained for two limits, the fast transitions (red) termed inner solution or threshold reduction, and the slow outer solutions (blue).

in a more rigorous way. To do this, the bifurcations in the reduced model must be analyzed and generic models of these bifurcation can be considered as qualitative descriptions of SD. A generic rate function of the activator would for example be a cubic polynomial, resulting in two stable states and a threshold (cf. Section III B).

To obtain a generic rate function of the inhibitor, one needs to analyze the reduced conductance based model when the ion gain via some reservoir is not treated as a bifurcation parameter. Then the onset of a cyclic SD process is caused by a subcritical Neimark–Sacker bifurcation from a state of tonic firing⁴¹. When neglecting the fast time scale of tonic firing, the subcritical Neimark–Sacker reduces to a subcritical Hopf bifurcation, corresponding to type II excitability (if we adopt the classification scheme from action potentials to SD). Hence, this justifies—in hindsight—the use of models showing such type II excitability for SD, as described in Section III B. Note however, that the model Eqs. (9)-(10) shows type II excitability with a supercritical Hopf bifurcation and subsequent canard explosion.

While this is still work in progress, such reduction techniques open up a systematic study of the bifurcation structure as a valuable diagnostic method to understand activation and inhibition of a new excitability in ion homeostasis which emerges in HH models with dynamic ion concentrations. This provides the missing link between the HH formalism and activator–inhibitor models that have been successfully used for modeling peri-infarct depolarizations and migraine phenotypes.

IV. CONCLUSIONS AND OUTLOOK

Spreading depression is the substrate of the migraine aura, and enhances infarct growth into the penumbra in stroke. The complex interplay of neuronal, homeostatic and metabolic dynamics in SD and peri-infarct depolarizations hampers the interpretation of pharmacological experiments. We discussed the basic (patho)physiology and biophysics of SD. Since these are largely known, most open questions on SD¹⁵ pertain the dynamics, interaction and relative contribution of the processes involved. In order to answer these, mathematical modeling is a useful and necessary tool. Many computational and mathematical models have been constructed, both biophysical and more abstract reaction–diffusion models, which have given insight in local ion dynamics, propagation mechanisms and pattern formation of SD.

Single cell conductance based models were discussed, which allow to study the local dynamics of intra- and extracellular ion concentrations and the neuronal membrane voltage during depolarization. In order to study SD propagation, a sheet of single cell models with extracellular spaces connected by diffusion can be constructed. While these are suitable for in silico experimentation, better insight in the mechanisms of initiation, propagation and pattern formation can be obtained by using general reaction-diffusion equations of activator–inhibitor type.

The RD activator–inhibitor models, in turn, have the disadvantage of not describing the underlying microscopic processes. To investigate how microscopic interactions of e.g. ion channels and drugs determine the occurrence and propagation of SD, conductance based single cell models can be reduced or linked to a general form that can be analyzed analytically. While it was discussed that in the HH model with dynamic ion concentrations the extracellular potassium concentration and potassium buffering are linked to respectively the activator and the inhibitor, a general method for making such a reduction is still work in progress. In addition, the long range interactions responsible for confining the spatial extent of SD, for which functional hyperemia and long range synaptic connections have been suggested as candidates, still need to be identified.

An important next step in modeling the spatial spread of SD in migraine is to include regional heterogeneity of the cerebral cortex. The cortex is not simply a 2D surface, but is a sheet with thickness variations and further areal, laminar, and cellular heterogeneity. The problem of SD spread in an individual person can therefore ultimately only be resolved in a neural tissue simulation that extends the requirements and constraints of circuit simulation methods on a cortical sheet by creating a tissue coordinate system that allows for geometrical analysis^{101,102}. Since the cortical heterogeneity is to some extent like a fingerprint an individual feature of each migraine sufferer, the goal in the future will be to upload patient’s MRI scanner readings into neural tissue

simulators that then can deliver the same output as clinical data. This can be used as a test bed for exploring the development of stereotactic neuromodulation.

A next step for modeling SD in ischemia, is analyzing both detailed^{79,103} and more phenomenological models^{104–106} that include energy availability, to identify the key factors that determine frequency and duration of SD's. Reducing SD after stroke and global ischemia is a potential target for therapy⁴. For example, patients with global ischemia (and trials in focal ischemia are ongoing^{107,108}) can benefit from mild therapeutic hypothermia¹⁰⁹. A possible mechanism is a reduced occurrence of SD. Analyzing SD dynamics during ischemia can not only help in selecting potential targets for neuroprotective agents or therapies, but also clarify the corresponding time window for successful application and elucidate critical differences between animal stroke models and human patients. These are key factors for the development of new neuroprotective drugs¹¹⁰.

In conclusion, modeling allows to further analyze the complex, dynamical phenomenon that is SD and can thereby aid in developing new treatments for migraine and stroke patients.

V. ACKNOWLEDGMENTS

The authors would like to thank the Fields Institute for hosting the workshop on Cortical Spreading Depression and Related Neurological Phenomena, allowing us to incorporate new recent insights in this review.

REFERENCES

- ¹Note1, the term spreading depolarization is sometimes used to distinguish between the wave in the tissue, and the observed depression of neuronal electrical activity or EEG signal. During severe hypoxia, for example, the EEG signal is already flat and therefore SD cannot depress it.
- ²A. A. P. Leão, *J Neurophysiol* **10**, 409 (1947).
- ³J. P. Dreier, *Nat Med* **17**, 439 (2011), URL <http://dx.doi.org/10.1038/nm.2333>.
- ⁴M. Lauritzen, J. P. Dreier, M. Fabricius, J. A. Hartings, R. Graf, and A. J. Strong, *J Cereb Blood Flow Metab* **31**, 17 (2011), URL <http://dx.doi.org/10.1038/jcbfm.2010.191>.
- ⁵M. Leonardi and A. Raggi, *Neurol. Sci.* **34 Suppl 1**, S117 (2013).
- ⁶H. Nakamura, A. J. Strong, C. Dohmen, O. W. Sakowitz, S. Vollmar, M. Su, L. Kracht, P. Hashemi, R. Bhatia, T. Yoshimine, et al., *Brain* **133**, 1994 (2010), URL <http://dx.doi.org/10.1093/brain/awq117>.
- ⁷J. A. Hartings, T. Watanabe, M. R. Bullock, D. O. Okonkwo, M. Fabricius, J. Woitzik, J. P. Dreier, A. Puccio, L. A. Shutter, C. Pahl, et al., *Brain* **134**, 1529 (2011).
- ⁸Y. B. Zeldovich and D. A. Frank-Kamenetskii, *Zh. Fiz. Khim.* **12, No. 1**, 100105 (1938).
- ⁹N. Wiener and A. Rosenblueth, *Arch. Inst. Cardiol. Mexico* **16**, 205 (1946).
- ¹⁰N. A. Trayanova, *Circ. Res.* **108**, 113 (2011).
- ¹¹D. DiFrancesco and D. Noble, *Philosophical Transactions of the Royal Society of London. B, Biological Sciences* **307**, 353 (1985).
- ¹²S. Dokos, B. Celler, and N. Lovell, *Annals of biomedical engineering* **21**, 321 (1993).
- ¹³D. Noble and Y. Rudy, *Philosophical Transactions of the Royal Society of London. Series A: Mathematical, Physical and Engineering Sciences* **359**, 1127 (2001).
- ¹⁴G. G. Somjen, *Physiol Rev* **81**, 1065 (2001).
- ¹⁵D. Pietrobon and M. A. Moskowitz, *Nat Rev Neurosci* **15**, 379 (2014), URL <http://dx.doi.org/10.1038/nrn3770>.
- ¹⁶B.-J. Zandt, Ph.D. thesis, University of Twente (2014).
- ¹⁷B.-J. Zandt, T. Stigen, B. Ten Haken, T. Netoff, and M. J. A. M. van Putten, *J Neurophysiol* **110**, 1469 (2013), URL <http://dx.doi.org/10.1152/jn.00250.2013>.
- ¹⁸C. Howarth, P. Gleeson, and D. Attwell, *J Cereb Blood Flow Metab* **32**, 1222 (2012), URL <http://dx.doi.org/10.1038/jcbfm.2012.35>.
- ¹⁹J. Keener and J. Sneyd, *Mathematical Physiology: I: Cellular Physiology, Interdisciplinary Applied Mathematics* (Springer, 2010), ISBN 9780387758473, URL <http://books.google.nl/books?id=n01mr5fs8I0C>.
- ²⁰N. Hübel, E. Schöll, and M. A. Dahlem, *PLoS Comput. Biol.* **10**, e1003551 (2014).
- ²¹R. Plonsey and R. C. Barr, *Bioelectricity* (Springer, 2007), 3rd ed.
- ²²M. J. A. M. van Putten, *Essentials of Neurophysiology - Basic Concepts and Clinical Applications for Scientists and Engineers* (Springer, 2009), URL <http://www.springer.com/engineering/biomedical+engineering/book/978-3-540-69889-0>.
- ²³P. G. Aitken, J. Jing, J. Young, and G. G. Somjen, *Brain Res* **541**, 7 (1991).
- ²⁴H. Kager, W. J. Wadman, and G. G. Somjen, *J Neurophysiol* **84**, 495 (2000).
- ²⁵B.-J. Zandt, B. ten Haken, J. G. van Dijk, and M. J. A. M. van Putten, *PLoS One* **6**, e22127 (2011), URL <http://dx.doi.org/10.1371/journal.pone.0022127>.
- ²⁶W. Yao, H. Huang, and R. M. Miura, *Bull Math Biol* **73**, 2773 (2011), URL <http://dx.doi.org/10.1007/s11538-011-9647-3>.
- ²⁷B.-J. Zandt, B. ten Haken, and M. J. A. M. van Putten, *J Neurosci* **33**, 5915 (2013), URL <http://dx.doi.org/10.1523/JNEUROSCI.5115-12.2013>.
- ²⁸T. Bastug and S. Kuyucak, *Chemical Physics Letters* **408**, 84 (2005), ISSN 0009-2614, URL <http://www.sciencedirect.com/science/article/pii/S0009261405005282>.
- ²⁹L. G. Longworth, *Journal of the American Chemical Society* **75**, 5705 (1953), ISSN 0002-7863, URL <http://dx.doi.org/10.1021/ja01118a065>.
- ³⁰C. Nicholson and J. M. Phillips, *J Physiol* **321**, 225 (1981).
- ³¹C. Nicholson and E. Syková, *Trends Neurosci* **21**, 207 (1998).
- ³²E. Syková and C. Nicholson, *Physiol Rev* **88**, 1277 (2008), URL <http://dx.doi.org/10.1152/physrev.00027.2007>.
- ³³B. Hille, *Ionic Channels of Excitable Membranes* (Sinauer Associates, Incorporated, 2001), ISBN 9780878932111, URL <http://books.google.nl/books?id=8VvK-QwAACAAJ>.
- ³⁴Y. Mori, *A multidomain model for ionic electrodiffusion and osmosis with an application to cortical spreading depression*, <http://arxiv.org/abs/1410.8391> (2014), arXiv:1410.8391.
- ³⁵A. C. G. Almeida, H. Z. Teixeira, M. A. Duarte, and A. F. C. Infantesi, *IEEE Trans Biomed Eng* **51**, 450 (2004), URL <http://dx.doi.org/10.1109/TBME.2003.821010>.
- ³⁶N. Qian and T. Sejnowski, *Biol Cybern* **62**, 1 (1989).
- ³⁷F. Helfferich and M. Plesset, *Ion Exchange Kinetics. A Nonlinear Diffusion Problem* (1958), URL <http://authors.library.caltech.edu/5628/2/HELjcp58corr.pdf>.
- ³⁸G. G. Somjen, *Ions in the Brain - Normal Function, Seizures, and Stroke* (Oxford University Press, 2004), chap. 18.
- ³⁹H. G. Glitsch, *Physiol Rev* **81**, 1791 (2001).
- ⁴⁰J. C. Skou, *Q Rev Biophys* **7**, 401 (1974).
- ⁴¹N. Hübel and M. A. Dahlem, in press: *PLoS Comp. Biol.* (2014).
- ⁴²J. Makarova, J. M. Ibarz, S. Canals, and O. Herreras, *Biophys J* **92**, 4216 (2007), URL <http://dx.doi.org/10.1529/biophysj>.

- 106.090332.
- ⁴³Note2, “Neural activity” is an ill-defined term. In neurovascular coupling, the term encompasses activity of the synapses, mitochondria and generation of action potentials.
- ⁴⁴M. Zonta, M. C. Angulo, S. Gobbo, B. Rosengarten, K.-A. Hossmann, T. Pozzan, and G. Carmignoto, *Nat Neurosci* **6**, 43 (2003), URL <http://dx.doi.org/10.1038/nn980>.
- ⁴⁵C. M. Anderson and M. Nedergaard, *Trends Neurosci* **26**, 340 (2003), URL [http://dx.doi.org/10.1016/S0166-2236\(03\)00141-3](http://dx.doi.org/10.1016/S0166-2236(03)00141-3).
- ⁴⁶C. Iadecola and M. Nedergaard, *Nat Neurosci* **10**, 1369 (2007), URL <http://dx.doi.org/10.1038/nn2003>.
- ⁴⁷S. Mangia, F. Giove, I. Tkci, N. K. Logothetis, P.-G. Henry, C. A. Olman, B. Maraviglia, F. Di Salle, and K. Uebachs, *J Cereb Blood Flow Metab* **29**, 441 (2009), URL <http://dx.doi.org/10.1038/jcbfm.2008.134>.
- ⁴⁸H. Farr and T. David, *J Theor Biol* **286**, 13 (2011), URL <http://dx.doi.org/10.1016/j.jtbi.2011.07.006>.
- ⁴⁹C. Ayata, *Stroke* **44**, S87 (2013), URL <http://dx.doi.org/10.1161/STROKEAHA.112.680264>.
- ⁵⁰C. T. Drake and C. Iadecola, *Brain Lang* **102**, 141 (2007), URL <http://dx.doi.org/10.1016/j.bandl.2006.08.002>.
- ⁵¹R. C. Sotero and N. J. Trujillo-Barreto, *Neuroimage* **39**, 290 (2008), URL <http://dx.doi.org/10.1016/j.neuroimage.2007.08.001>.
- ⁵²W. J. Pearce, *Pharmacol Ther* **65**, 75 (1995).
- ⁵³U. Dirnagl and W. Pulsinelli, *J Cereb Blood Flow Metab* **10**, 327 (1990), URL <http://dx.doi.org/10.1038/jcbfm.1990.61>.
- ⁵⁴B. E. Lindquist and C. W. Shuttleworth, *Neuroscience* **223**, 365 (2012), URL <http://dx.doi.org/10.1016/j.neuroscience.2012.07.053>.
- ⁵⁵S. C. Schock, N. Munyao, Y. Yakubchuk, L. A. Sabourin, A. M. Hakim, E. C. G. Ventureyra, and C. S. Thompson, *Brain Res* **1168**, 129 (2007), URL <http://dx.doi.org/10.1016/j.brainres.2007.06.070>.
- ⁵⁶K. B. Churchwell, S. H. Wright, F. Emma, P. A. Rosenberg, and K. Strange, *J Neurosci* **16**, 7447 (1996).
- ⁵⁷E. K. Hoffmann, I. H. Lambert, and S. F. Pedersen, *Physiol Rev* **89**, 193 (2009), URL <http://dx.doi.org/10.1152/physrev.00037.2007>.
- ⁵⁸M. Müller and G. G. Somjen, *J Neurophysiol* **83**, 735 (2000).
- ⁵⁹B. E. Shapiro, *J Comput Neurosci* **10**, 99 (2001).
- ⁶⁰J. Hofmeijer and M. J. A. M. van Putten, *Stroke* **43**, 607 (2012), URL <http://dx.doi.org/10.1161/STROKEAHA.111.632943>.
- ⁶¹J. J. Hablitz and U. Heinemann, *Brain Res Dev Brain Res* **46**, 243 (1989).
- ⁶²J. P. Dreier, S. Major, H.-W. Pannek, J. Woitzik, M. Scheel, D. Wiesenthal, P. Martus, M. K. L. Winkler, J. A. Hartings, M. Fabricius, et al., *Brain* **135**, 259 (2012).
- ⁶³Note3, for completeness, we mention the cellular automata model of ϕ , who model tissue as a grid of machines, that turn on and off depending on the state of their neighbors. The propagation of activity in such a grid is very similar to the propagation of reaction-diffusion waves. The automata are a computationally efficient method for numerically investigating propagation of RD waves in complex geometries. Due to the lack of congruence with physiological mechanisms of SD, this approach has recently seen little interest in SD research.
- ⁶⁴M. Vincent and N. Hadjikhani, *Cephalalgia* **27**, 1368 (2007).
- ⁶⁵R. M. Miura, H. Huang, and J. J. Wylie, *Chaos* **23**, 046103 (2013), URL <http://dx.doi.org/10.1063/1.4821955>.
- ⁶⁶E. Barreto and J. R. Cressman, *J Biol Phys* **37**, 361 (2011), URL <http://dx.doi.org/10.1007/s10867-010-9212-6>.
- ⁶⁷J. R. Cressman, G. Ullah, J. Ziburkus, S. J. Schiff, and E. Barreto, *J Comput Neurosci* **26**, 159 (2009), URL <http://dx.doi.org/10.1007/s10827-008-0132-4>.
- ⁶⁸J. R. Cressman, G. Ullah, J. Ziburkus, S. J. Schiff, and E. Barreto, *J Comput Neurosci* (2011), URL <http://dx.doi.org/10.1007/s10827-011-0333-0>.
- ⁶⁹H. Kager, W. J. Wadman, and G. G. Somjen, *J Neurophysiol* **88**, 2700 (2002), URL <http://dx.doi.org/10.1152/jn.00237.2002>.
- ⁷⁰H. Kager, W. J. Wadman, and G. G. Somjen, *J Comput Neurosci* **22**, 105 (2007), URL <http://dx.doi.org/10.1007/s10827-006-0001-y>.
- ⁷¹M. Bazhenov, I. Timofeev, F. Fröhlich, and T. J. Sejnowski, *Drug Discov Today Dis Models* **5**, 45 (2008), URL <http://dx.doi.org/10.1016/j.ddmod.2008.07.005>.
- ⁷²G. Florence, M. A. Dahlem, A.-C. G. Almeida, J. W. M. Bassani, and J. Kurths, *J Theor Biol* **258**, 219 (2009), URL <http://dx.doi.org/10.1016/j.jtbi.2009.01.032>.
- ⁷³G. G. Somjen, H. Kager, and W. J. Wadman, *J Comput Neurosci* **26**, 139 (2009), URL <http://dx.doi.org/10.1007/s10827-008-0103-9>.
- ⁷⁴G. P. Krishnan and M. Bazhenov, *J Neurosci* **31**, 8870 (2011), URL <http://dx.doi.org/10.1523/JNEUROSCI.6200-10.2011>.
- ⁷⁵L. Øyehaug, I. Østby, C. M. Lloyd, S. W. Omholt, and G. T. Einevoll, *J Comput Neurosci* **32**, 147 (2012), URL <http://dx.doi.org/10.1007/s10827-011-0345-9>.
- ⁷⁶H. C. Tuckwell and R. M. Miura, *Biophys J* **23**, 257 (1978), URL [http://dx.doi.org/10.1016/S0006-3495\(78\)85447-2](http://dx.doi.org/10.1016/S0006-3495(78)85447-2).
- ⁷⁷H. C. Tuckwell, *Int J Neurosci* **10**, 145 (1980).
- ⁷⁸H. Z. Teixeira, A.-C. G. de Almeida, A. F. C. Infantosi, M. A. Vasconcelos, and M. A. Duarte, *J Neural Eng* **1**, 117 (2004), URL <http://dx.doi.org/10.1088/1741-2560/1/2/007>.
- ⁷⁹M.-A. Dronne, J.-P. Boissel, and E. Grenier, *J Theor Biol* **240**, 599 (2006), URL <http://dx.doi.org/10.1016/j.jtbi.2005.10.023>.
- ⁸⁰G. Ullah, J. R. Cressman, Jr, E. Barreto, and S. J. Schiff, *J Comput Neurosci* **26**, 171 (2009), URL <http://dx.doi.org/10.1007/s10827-008-0130-6>.
- ⁸¹H. C. Tuckwell, *Int J Neurosci* **12**, 95 (1981).
- ⁸²D. Postnov, D. Postnov, and L. Schimansky-Geier, *Brain research* **1434**, 200 (2012).
- ⁸³B. Grafstein, in *Brain Function. Cortical Excitability and Steady Potentials*, edited by M. A. B. Brazier (University of California Press, Berkeley, 1963), pp. 87–124.
- ⁸⁴J. Bureš, O. Burešová, and J. Křivánek, *The mechanism and applications of Leão's Spreading Depression* (Academia, New York, 1974).
- ⁸⁵U. Heinemann and H. D. Lux, *Brain Res* **120**, 231 (1977).
- ⁸⁶I. Idris and V. N. Biktashev, *Phys Rev Lett* **101**, 244101 (2008).
- ⁸⁷J. A. Reggia and D. Montgomery, *Proc. Annu. Symp. Comput. Appl. Med. Care* pp. 873–877 (1994).
- ⁸⁸J. A. Reggia and D. Montgomery, *Comput. Biol. Med.* **26**, 133 (1996).
- ⁸⁹K. Lashley, *Arch. Neurol. Psychiatry* **46**, 331 (1941).
- ⁹⁰W. Richards, *Sci. Am.* **224**, 88 (1971).
- ⁹¹R. Kapral and K. Showalter, eds., *Chemical Waves and Patterns* (Kluwer, Dordrecht, 1995).
- ⁹²M. A. Dahlem and S. C. Müller, *Ann. Phys.* **13**, 442 (2004).
- ⁹³M. A. Dahlem and N. Hadjikhani, *PLoS ONE* **4**, e5007 (2009).
- ⁹⁴A. C. Charles and S. M. Baca, *Nat. Rev. Neurol.* (2013).
- ⁹⁵M. A. Dahlem and T. M. Isele, *J. Math. Neurosci* **3**, 7 (2013).
- ⁹⁶C. Ayata, *Headache: The Journal of Head and Face Pain* **50**, 725 (2010), ISSN 1526-4610.
- ⁹⁷K. Krischer and A. S. Mikhailov, *Phys. Rev. Lett.* **73**, 3165 (1994).
- ⁹⁸R. Woesler, P. Schütz, M. Bode, M. Or-Guil, and H.-G. Purwins, *Physica D: Nonlinear Phenomena* **91**, 376 (1996).
- ⁹⁹C. Schenk, M. Or-Guil, M. Bode, and H.-G. Purwins, *Physical Review Letters* **78**, 3781 (1997).
- ¹⁰⁰E. J. Doedel and B. E. Oldeman, *Auto-07P: Continuation and bifurcation software for ordinary differential equations*, Concordia University, Montreal, Canada (2009).
- ¹⁰¹J. Kozloski and J. Wagner, *Frontiers in neuroinformatics* **5** (2011).
- ¹⁰²M. A. Dahlem, B. Schmidt, I. Bojak, S. Boie, F. Kneer, N. Hadjikhani, and J. Kurths, *Tech. Rep.*, PeerJ PrePrints (2014).

- ¹⁰³M.-A. Dronne, E. Grenier, G. Chapuisat, M. Hommel, and J.-P. Boissel, *Prog Biophys Mol Biol* **97**, 60 (2008), URL <http://dx.doi.org/10.1016/j.pbiomolbio.2007.10.001>.
- ¹⁰⁴K. Revett, E. Ruppin, S. Goodall, and J. A. Reggia, *J Cereb Blood Flow Metab* **18**, 998 (1998), URL <http://dx.doi.org/10.1097/00004647-199809000-00009>.
- ¹⁰⁵L. Vatov, Z. Kizner, E. Ruppin, S. Meilin, T. Manor, and A. Mayevsky, *Bull Math Biol* **68**, 275 (2006), URL <http://dx.doi.org/10.1007/s11538-005-9008-1>.
- ¹⁰⁶G. Chapuisat, M.-A. Dronne, E. Grenier, M. Hommel, and J.-P. Boissel, *Acta Biotheor* **58**, 171 (2010), URL <http://dx.doi.org/10.1007/s10441-010-9100-2>.
- ¹⁰⁷H. B. van der Worp, M. R. Macleod, R. Kollmar, and E. S. R. N. f. H. E. Y. P. , *J Cereb Blood Flow Metab* **30**, 1079 (2010).
- ¹⁰⁸U.S. National Institutes of Health, *The intravascular cooling in the treatment of stroke 2/3 trial (ictus2/3)* (2014), <http://clinicaltrials.gov/show/NCT01123161>, acc.: 6-10-2014.
- ¹⁰⁹N. Nielsen, J. Wetterslev, T. Cronberg, D. Erlinge, Y. Gasche, C. Hassager, J. Horn, J. Hovdenes, J. Kjaergaard, M. Kuiper, et al., *New England Journal of Medicine* **369**, 2197 (2013), PMID: 24237006, <http://www.nejm.org/doi/pdf/10.1056/NEJMoa1310519>, URL <http://www.nejm.org/doi/full/10.1056/NEJMoa1310519>.
- ¹¹⁰G. Z. Feuerstein and J. Chavez, *Stroke* **40**, S121 (2009), URL <http://dx.doi.org/10.1161/STROKEAHA.108.535104>.